



FOULING OF COMBUSTION CHAMBERS AND HIGH-TEMPERATURE FILTERS

J. D. Isdale,* A. M. Jenkins,* V. Semião,† M. G. Carvalho‡ and M. C. Welbourne‡

*National Engineering Laboratory, East Kilbride, Glasgow, G75 0QU, UK, †Instituto Superior Técnico, 1096, Lisboa, Portugal and ‡Rolls Royce International Combustion Ltd, Derby, DE2 9GJ, UK

Abstract—This paper provides a summary of the main topics which contribute to a major study aimed at integrating fouling and combustion activities for application to furnaces and filters. Brief outlines of the aims of the seven main activities are provided along with typical examples of some of the results from furnace modelling, deposit structure and properties simulations, industrial measurement and filtration studies. Application of the results will lead to improved energy efficiency in aspects of furnace and filter performance. Crown copyright © 1997 Published by Elsevier Science Ltd.

Keywords—Combustion, fouling, energy efficiency, filters.

INTRODUCTION

For both combustion chambers and filters, similar sets of deposition mechanisms, active in higher-temperature regimes, interact with the efficiency of the process [1]. For furnaces, the mechanisms produce deposits on the walls, which reduce heat transfer, and so influence the combustion reactions; for high-temperature filters they are the controlling physical phenomena which determine how effectively the filter will function and how rapidly it will become clogged.

Current demands for better energy efficiency and environmental control in the process industries have emphasised the need for better understanding of all types of thermal process to optimise both energy utilisation and environmental emissions. Within this study, models for these have been derived from theoretical and analytic studies in combination with experimental and computational fluid dynamics (CFD) exercises to provide the necessary data and parameters for industrial plant.

This study has extended the results of earlier work [2–4] and has included both experimental and theoretical studies of a furnace configuration and a high-temperature filtration system. The complete project aimed to provide methods to determine the influence of fouling mechanisms on combustion processes and high-temperature filters and so contributed to the design and operation of these facilities throughout the process industries.

To improve the accuracy of the calculations for heat release within a furnace and the heat available at the furnace exit, two new aspects were added to existing modelling approaches. Near-wall velocity, temperature and particle distribution fields, as well as fouling, were taken into account. This study took the approach of using a general model for the bulk flow, based on CFD codes including a new submodel for particulate formation and transport, and another model optimised for the wall region. The latter was based on the ‘absence of turbulence model’ using a direct numerical simulation (DNS) approach, which eliminated the need for non-universal ‘wall functions’ [5].

Since fouling processes also arise from the complex interaction of a number of physical and chemical processes, new models to predict deposition rates for furnace walls and high-temperature filters were required. These have been derived from theoretical and analytic studies combined with measured experimental data from industrial plant.

For the complex surface and volume structures occurring in filters or loosely packed deposits, calculations of properties by conventional Newtonian mechanics are often inadequate

approximations and very computer intensive in time. Since properties are required for the heat transfer and other calculations, new methods have been developed at GCU based on scaling laws of multi-fractal geometry and appropriate Newtonian approximations, to provide the necessary data. The results were validated by comparison with process industry test data.

The participants in the project were National Engineering Laboratory, UK (NEL); Groupement pour la Recherche sur les Echangeurs Thermiques (GRETh), France; International Combustion Ltd, UK (IC); Glasgow Caledonian University, UK (GCU); and Instituto Superior Technico, Portugal (IST). Additional contributions have also been provided by other industrial collaborators where indicated.

FURNACE STUDIES

The aim of the study on furnaces has been to develop and apply appropriate techniques to calculate in particular those parameters which control fouling of the chamber walls. This was achieved by combining the two types of CFD approach outlined above with the experimental furnace studies outlined below. The coupling of the bulk and near wall modelling, however, is not direct, but is achieved via dimensionless friction velocity and kinematic viscosity.

Bulk modelling

The objective of the study carried out at IST was to develop a 3D CFD model, including combustion and radiative heat transfer, to analyse the gas flow close to the furnace walls, even within recirculation zones. Particulate formation, gas and particle velocities and temperatures for the furnace were considered, with special emphasis on the near wall regions.

The work has been carried out on three fronts. The first, two-dimensional two-phase modelling (2D) dealt with the axisymmetric arrangements of most fuelling devices and the second, 3D bulk modelling, represented industrial furnaces and combustors where the two-dimensional assumption was no longer valid. The inlet conditions for the axisymmetric predictions were given by the third calculation procedure, which provided numerical evaluation of the droplet size distribution as a function of the atomiser design and operating conditions.

The two-dimensional calculations aimed at the development of a physical model to simulate particulate formation for fuel-oil firing, for incorporation in the three-dimensional predictions. Both approaches required the numerical solution of elliptic-type equations for conservation of mass, momentum, energy and species concentrations. Turbulence was considered by using the $k-\epsilon$ model [6] and combustion by equilibrium-chemistry assumptions which involved the solution of equations for the mixture fraction and its fluctuations.

The work carried out included two-phase flow predictions, using a grid comprising 51×37 nodes, for velocity, temperature and species concentration throughout the furnace. Experimental measurements of furnace temperature profiles and of CO_2 and O_2 concentrations have been carried out and compared with model predictions. Corresponding predictions for fuel and soot concentrations have also been made.

For the three-dimensional bulk modelling of the IC furnace, velocity, temperature and species concentration calculations have been carried out for isothermal turbulent flow in several horizontal, transverse and longitudinal planes. These have been based on a $40 \times 44 \times 45$ node grid to characterise the velocity, temperature, density and species concentration fields and permit identification of recirculation zones. A Lagrangian model for cenospheres (coke particles) formation, oxidation and transport throughout the furnace was developed and included in the 3D general CFD code in order to quantify the particulate number distribution in the near wall region. The resulting particle tracks are illustrated in Fig. 1 for the IC furnace.

Since fouling is strongly dependent on the initial diameters of the droplets, a computer code capable of predicting the DSD (droplet size distribution) for several types of atomisers has also been developed. This code is able to predict the SMD (Sauter Mean Diameter) and the DSD for the most common atomisers, including pressure-jet, pre-filming airblast and plain-jet airblast types. The SMD, which is the characterising parameter for the DSD, is calculated by means of semi-empirical correlations. A comparison of the predicted SMD values for a pressure jet atomiser with experimental data from the literature is given in Fig. 2. For the two-phase flow calculations,

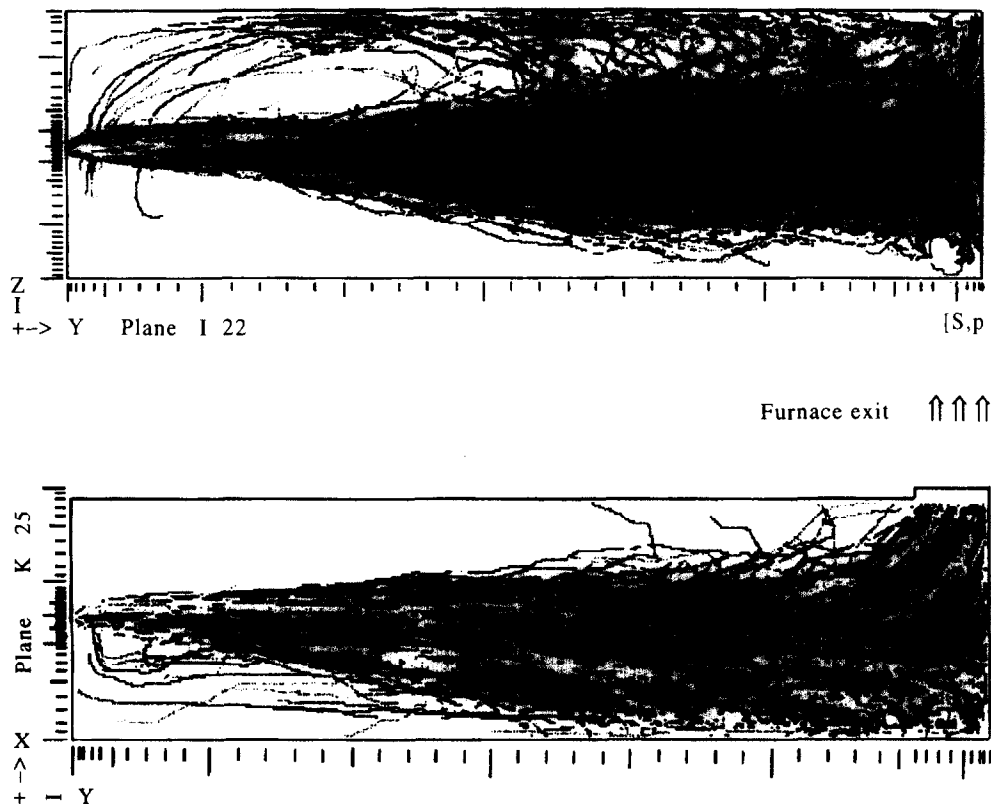


Fig. 1. Particle generation and tracking in IC furnace.

the droplets were tracked by means of a Lagrangian approach, with a stochastic model for the droplet trajectories.

Near wall modelling

The near wall modelling has also been carried out using CFD, but for this work the direct numerical simulation technique (DNS) [5] for confined geometries was used along with the GRETH TRIO code [7], which is particularly suitable for this purpose. Although 'wall functions' are commonly used in this situation, these are non-universal and do not provide sufficiently detailed access to those parameters which are crucial for the calculation of fouling. The objective of using the DNS approach was to provide instantaneous coupling of the fluid and particle motion, with results expressed in a non-dimensional form so that they can be related to the bulk modelling results. For the near wall case a small ($6 \times 6 \times 3$ mm) rectangular calculation domain was chosen, with a highly refined mesh to provide a good description of the main part of the turbulent structures. The mesh control volumes used were $80 \times 40 \times 45$, with linear mesh steps in two directions and a progressively decreasing step size perpendicular to the wall (reaching 20 mm in width next to the wall).

The main characteristic of the DNS approach to turbulent flow is that it produces non-stationary results, that is the flow field is different at each time step, with each result related to the previous one by solutions to the transient momentum balance. Consequently, a statistical averaging process was required in order to obtain time-averaged values of the main flow variables, such as velocity, pressure or temperature. To assess the code, a fully developed flow at 10 ms^{-1} was studied, with re-injection of velocity between the inlet and outlet faces of the calculation domain at each step at a re-injection time of 0.6 ms. Extensive analysis of the turbulence predicted by the code was carried out for comparison with corresponding data from the literature. This gave values in good accordance with other workers, however the turbulent structures predicted were complex and may have been influenced by the transverse boundary conditions.

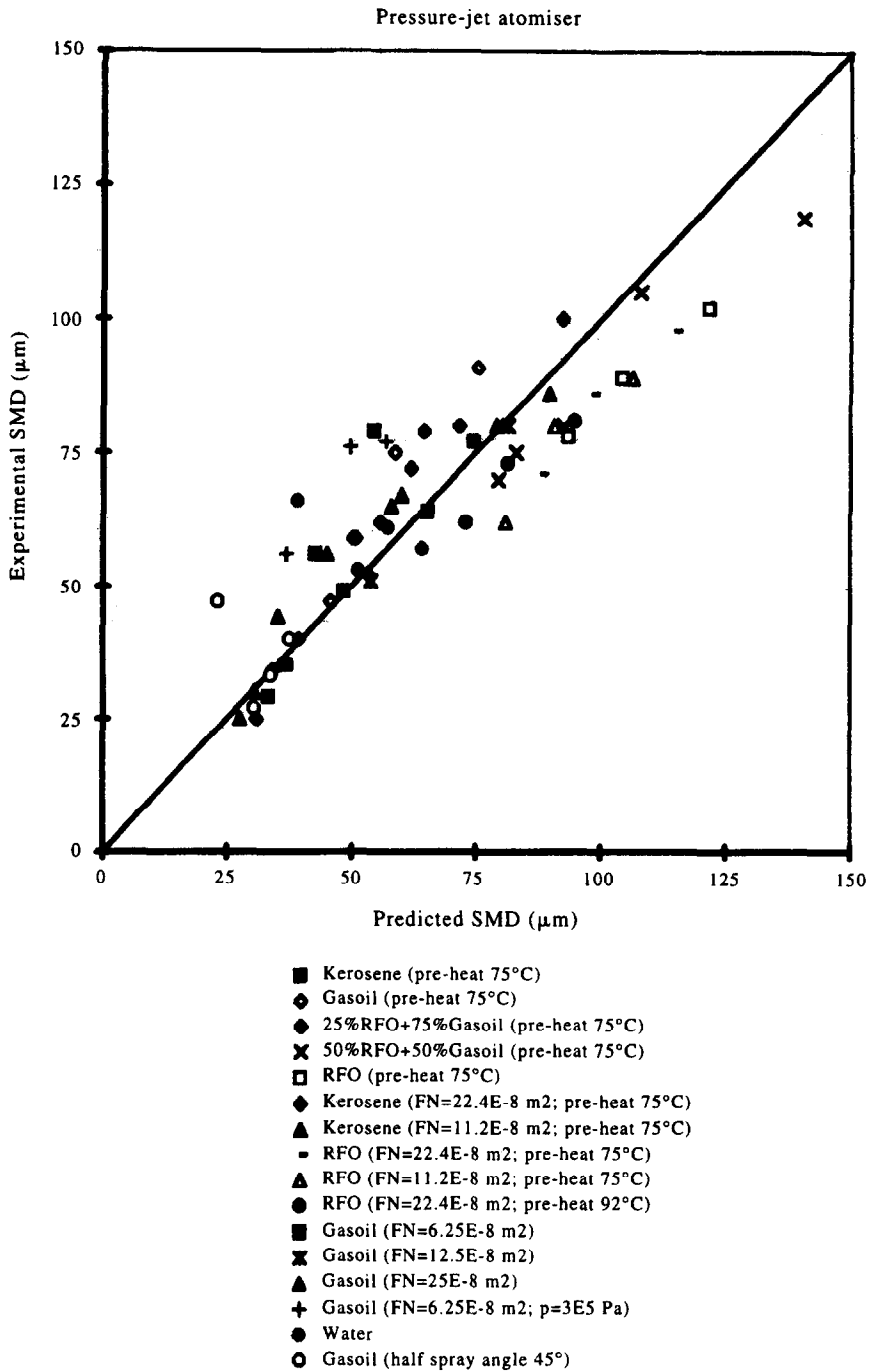


Fig. 2. Calculated and experimental Sauter Mean Diameter (SMD) for a range of fuels and nozzle flow numbers (FN).

FURNACE FOULING STUDIES

The aim of the work on fouling was to develop and apply appropriate methods to calculate net deposition rates on furnace walls. Together with industrial partners, the work aimed to provide predictive models which have been tested by direct comparison with data from operating industrial plant. The procedures developed at GCU use recent advances in the application of fractal dimensions to a wide range of areas. The work therefore included a combination of new deposition models, deposit property calculations and measured industrial experimental data.

Deposition rate modelling

Two-dimensional mathematical simulations have been carried out for deposition on a straight-line substrate and on a circular disc, to represent three-dimensional effects on walls and tubular surfaces. For this part of the work the geometry of the fouling was captured by the mass fractal dimension and the relative effect of each transport mechanism examined. Understanding of the relation between deposit structure and transport mechanisms was furthered by relating the fractal dimension to the formation mechanisms of the deposit. Various parameters of the process [8] were analysed to show the relative effects of each transport mechanism on the time-dependent growth of the deposit using identical particles with a sticking probability of one. Ratios of the different forces acting on the particles were derived from the transport mechanisms and used to determine the probability of the particle moving in each of the four possible directions. The unit sticking probability used for the simulation implies that all particles which impact are captured and hence a maximum deposition rate is calculated, but the structure of the deposit is not affected.

The simulation parameters were chosen to represent the effects of the streamlines, particle inertia, thermophoresis, diffusion and compaction of the deposit. For each simulation, particles were assigned a selected set of parameters before release at a prescribed height above the deposit, with the initial horizontal position chosen randomly. The parameters thus controlled the behaviour of the simulation and were dimensionless numerical constants, except for the initial velocity (measured in pixels per second CPU time), which was randomly chosen between zero and some maximum. A compaction factor (0 for no compaction and 1 for maximum compaction) was added to allow for additional effects which may be present in real systems (shape for example), as opposed to the numerical simulation which is here limited to pixel shape. A selection of the simulation parameters used is given in Table 1, with the corresponding simulated tube deposits shown in Fig. 3.

To provide a basis for comparison between simulations and experiments, the time-dependent growth of each deposit was examined using several quantities which could be directly obtained for the simulations (number of particles deposited, cumulative mass deposition rate, fractal dimension or density). The time variable used was the actual CPU time taken by the simulation as it progressed, which is related to the real time through the random values of the particle release parameters. Due to the contrasting nature of the growth on the front and back face of the disk these quantities were calculated separately.

In the simulation the particles are released in series and it was assumed that they travelled independently of one another with the only interaction occurring at the deposit surface.

A typical set of results is given in Fig. 4, which corresponds to the simulation shown in Fig. 3(i), which shows that there appears to be an approximately linear relationship between deposition rate and the fractal dimension above values of 1.3. As the simulation proceeded the mass deposition rate was calculated each time an additional 100 particles joined the deposit to obtain an indication of how the rate varied as the deposit grew. The fractal dimension was calculated using the box-counting method. Again this was conducted over the same intervals as the mass deposition rate to relate the two quantities, however more extensive sets of experiments are required before firm conclusions can be made on the connection between mechanisms forming the deposit and their fractal dimension.

Table 1. Dimensionless simulation parameters and results for Fig. 3

Simulation No.	(a)	(b)	(c)	(d)	(e)	(f)	(g)	(h)	(i)
Maximum velocity (pixels s ⁻¹)	2	2	2	2	2	2	2	2	2
Compaction factor	0	1	0.8	0.5	0.1	0.8	0.5	1	1
Transport force parameters	0								
Inertia	0		0	0	0.5	2.0	6.0	0.5	0.5
Hydrodynamic	0	2	5	10	1	5	1	1	5
Thermophoretic	0	0	0	0	0	0	0	0.5	0.5
Diffusion	1	1	1	1	1	0	1	1	1
Results									
Total CPU time (s)	741	935	586	424	1362	213	1256	1167	571
Deposited particles	1824	4493	4089	3961	5562	3572	5667	7193	4721
Released particles	10 000	10 000	10 000	10 000	10 000	10 000	10 000	10 000	10 000
Deposition rate (s ⁻¹)	2.468	4.807	6.974	9.351	4.083	16.75	4.510	6.164	8.268

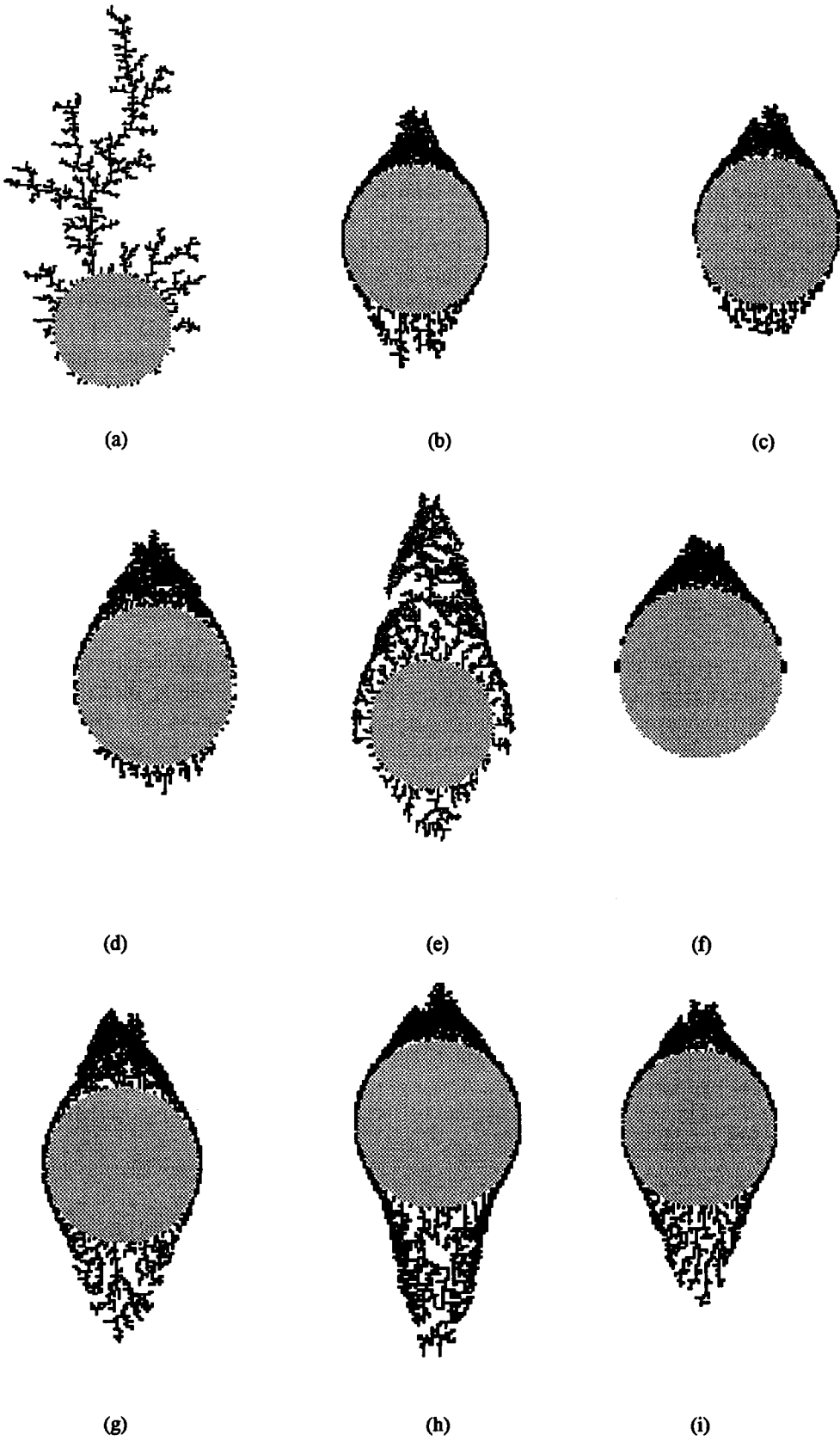


Fig. 3. Simulation of deposition on a probe surface cross-section.

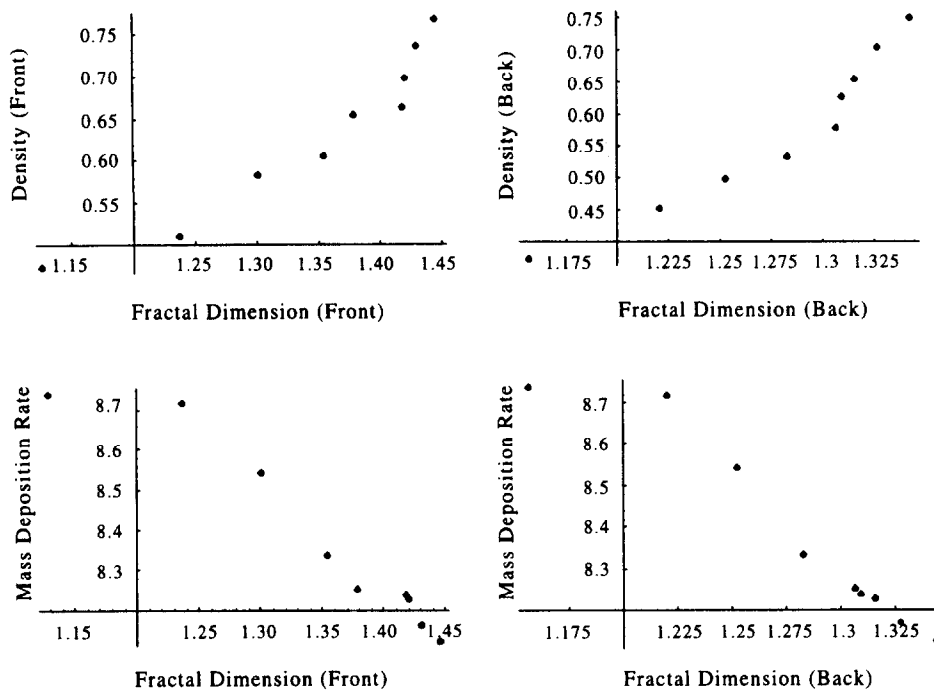


Fig. 4. Time dependencies of simulated probe deposit characteristics. The data above refer to the simulation shown in Fig. 3(i).

Deposit property modelling

Relating the mass fractal dimension to the physical properties of the deposit is potentially a very powerful predictive tool and the results for density are illustrated in Fig. 4. The effect of deposit geometry on its thermal conductivity was also examined for a two-dimensional cross-section using the fractal approach. The deposit fractal dimension captured the internal geometry of the deposit, which was then related to the thermal conductivity. This was achieved via a numerically determined shape factor, S [9], and the deposit porosity, e . The porosity was then in turn related to the fractal dimension, d , for the type of fractal used, to characterise the deposit [10], in this case a Sierpinski carpet. Scaling relationships between the conductivity and the relevant parameters have been extensively examined and excellent agreement obtained. The details of the explicit relationship between the two is the subject of a forthcoming publication [11].

Analyses of the temperature field distribution within the structure for the randomly generated deposits have also been carried out. This involved the production of solutions to Laplace's equation throughout the structures, a computationally intensive task for which programs typically ran for several days on a Silicon Graphics Indy workstation. Some typical deposits and their respective temperature field distributions are shown in Fig. 5. The level of grey scale indicates the temperature (white is hottest). Due to the coarseness of the grey scale discretisation and the dendritic nature of the deposits, the edges appear to have the same temperature as the gas stream. A further improvement to the temperature field calculation is planned which will include solutions to Laplace's equation, not only within the deposit but also within the gas phase. This will necessitate continuity conditions at the interface between the two phases and thus increase the computational complexity but it will provide a more realistic temperature distribution.

Experimental studies

Mass accumulation, heat flux and furnace temperature measurements have been made in a full-scale (88 MW) test facility at IC, using appropriate probes. The whole-furnace model was used to help select the locations for probe measurements. Selected tests were carried out at the different levels of load available (70, 40 and 26 MW) and for two different fuels, Orimulsion and a heavy

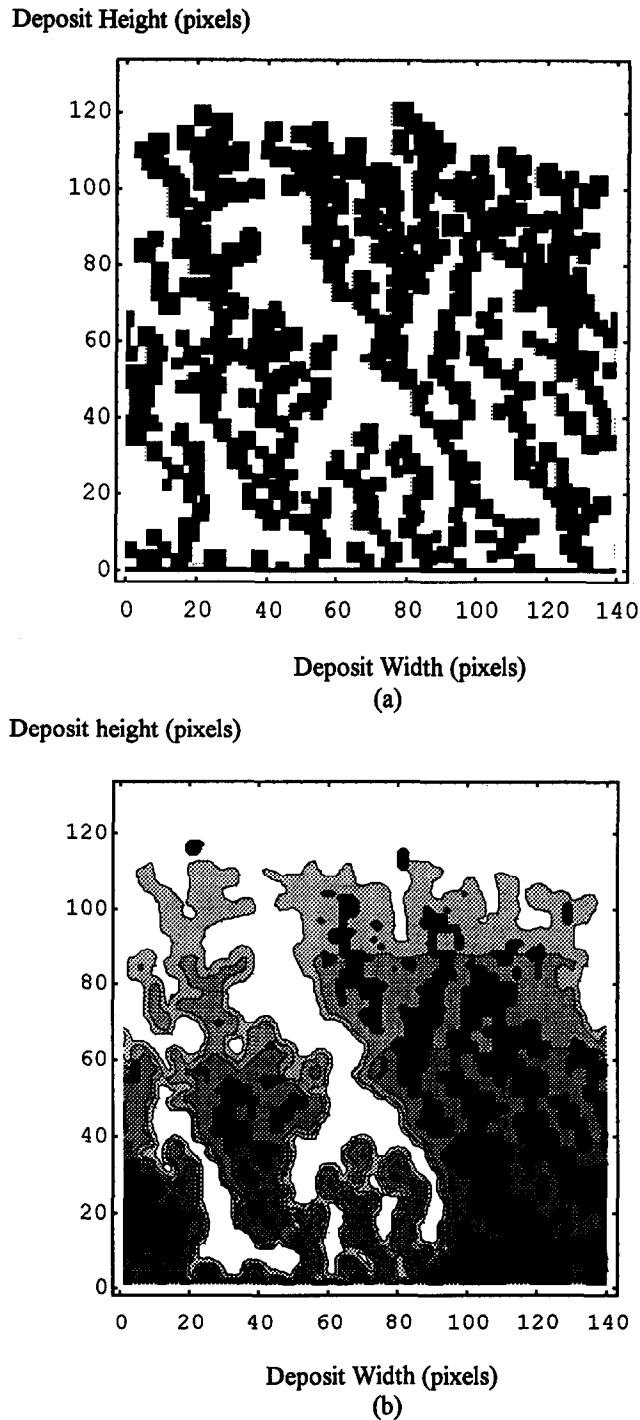


Fig. 5. Detail of simulated fouling deposit (a) and the corresponding calculated temperature distribution in the solid (b). White is gas-stream temperature; black is maximum solid temperature.

fuel oil (HFO). The data produced were used for development and validation of the furnace models and, in combination with additional data, for the fouling models as indicated below. Preliminary results of the deposition and heat flux measurements along the furnace are shown in Figs 6 and 7.

In addition, a specialised furnace deposition probe has been manufactured and used to carry out tests in a 30 MW front-wall-fired low NO_x burner of second-generation design. This incorporated both air and fuel staging, together with 'in-burner' recirculated flue gas to attenuate

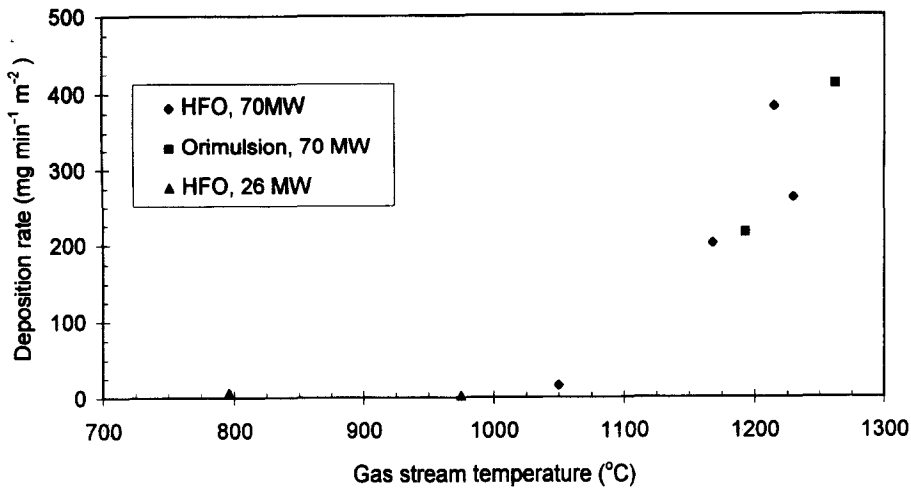


Fig. 6. Probe measurements of mass deposition in the IC furnace burning heavy fuel oil (HFO) and Orimulsion.

the flame and reduce both thermal and fuel-generated NO_x. The result of this staging was to reduce the flame temperature and produce an ash which is lighter and more friable. This probe was in the form of an air-cooled stainless-steel tube of 50 mm external diameter and approximately 3 m long. Tests to date have included measurements at two locations where the CFD analysis indicated a uniform flow, firstly remote from the burner (10 m downstream) and hidden from the burner radiation and, secondly, in the main combustion chamber. The former location gave a low probe temperature (maximum 650°C) and no significant fouling, while the second gave a probe metal temperature above 700°C and rapid deposit build up to a depth of 15 mm for 2 h of exposure. Further tests are being carried out to provide more data on these effects. The fuel used was a high-quality Polish coal, and probe deposits were examined by electron microscopy. This showed that the deposit was more compact at the tube surface than in the rest of the thickness and that the main deposit structures were themselves porous as well as discontinuous (and possibly fractal) in nature. An example is shown in Fig. 8. The lower micrograph of this figure is a detail of the lower right-hand section of the upper micrograph at higher magnification and the repetition of the porosity at different scales is evident.

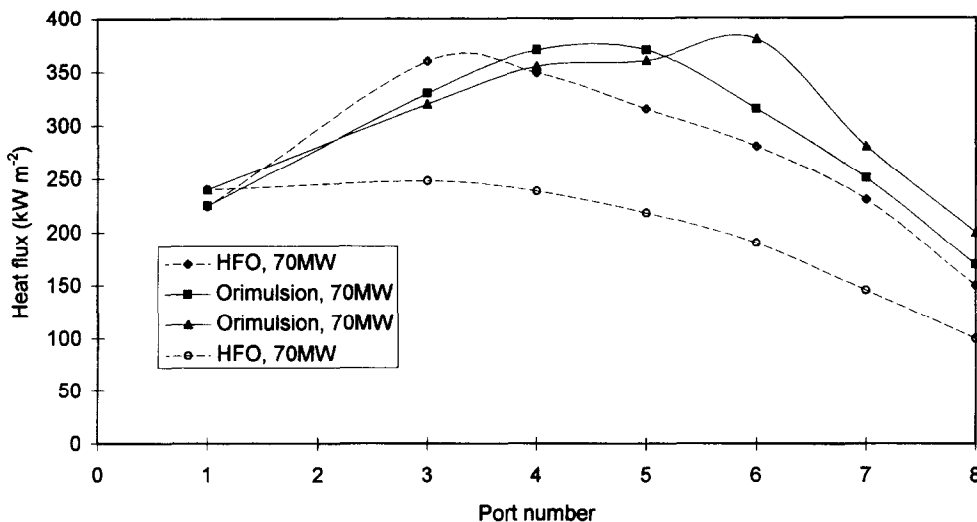


Fig. 7. Heat flux measurements at IC furnace burning heavy fuel oil (HFO) and Orimulsion.

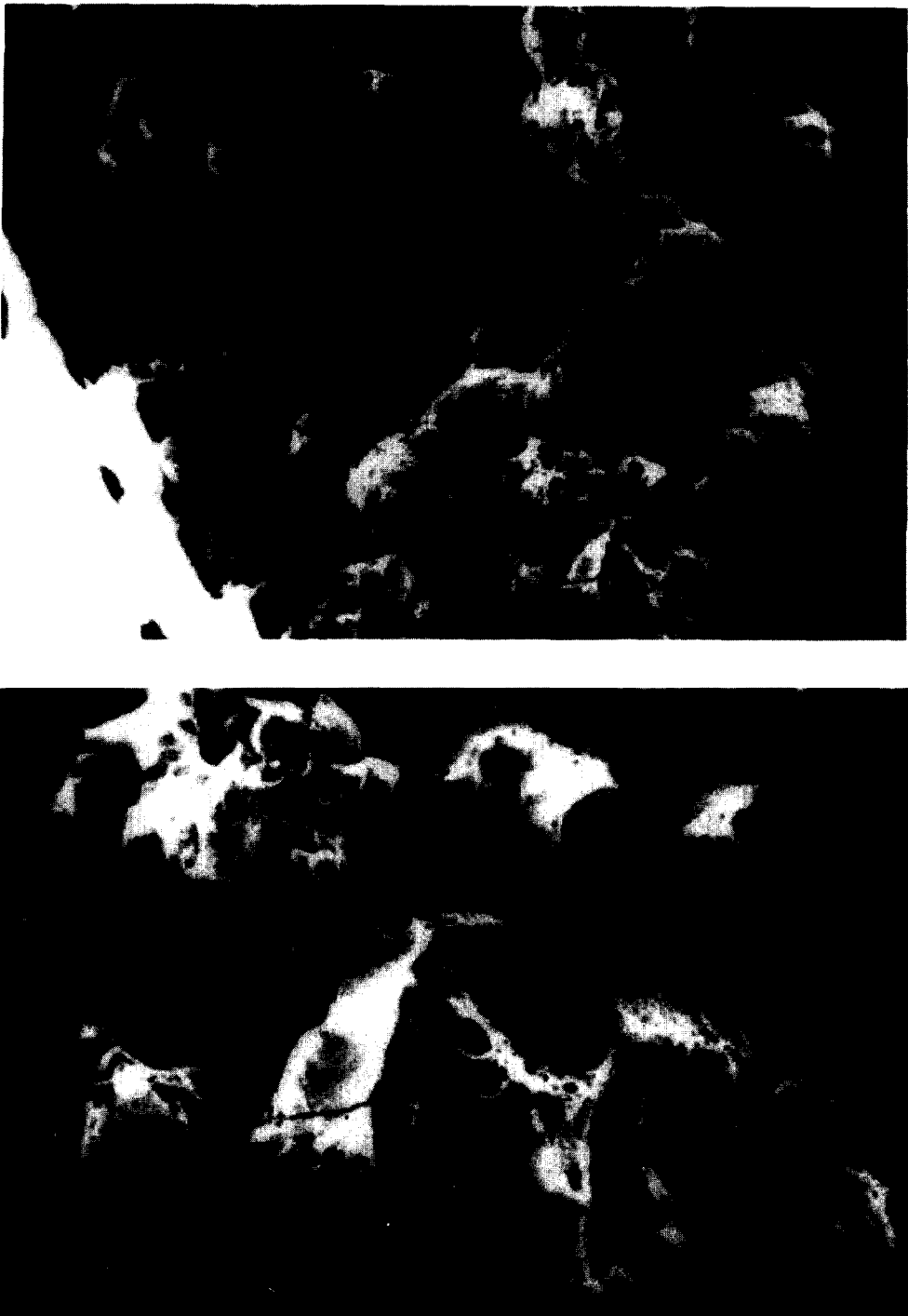


Fig. 8. Micrographs of furnace deposits. The lower micrograph is a detail of the lower right section of the upper.

FILTRATION STUDIES

The aim of this study was to develop novel methods for application to both deposit and filter structures and to produce data which can be used for validation. Mathematical models and simulations were employed which utilised fractal ideas to provide a clearer understanding of filter performance [12–15].

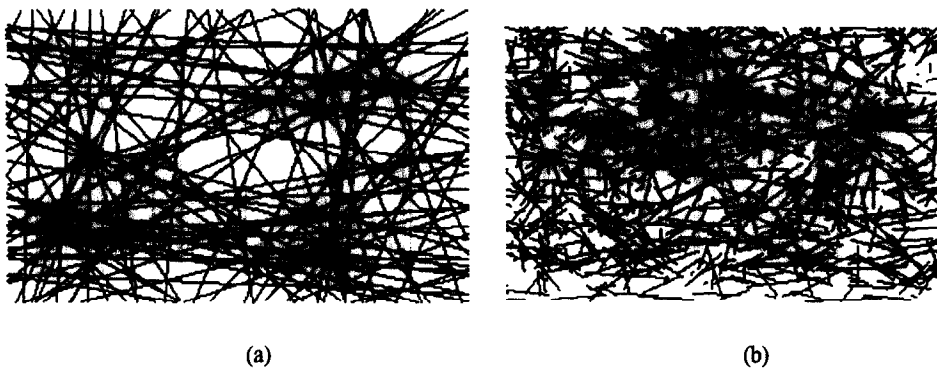


Fig. 9. Computer simulations of two fibrous membranes filters. Each fibre is randomly generated within a rectangle according to the following rules. A random point (x,y) within the rectangle and a random angle of orientation are chosen. the fibre is then placed through this point at the chosen angle of orientation. In (a), the length of the fibre is constrained only by the boundary of the rectangle (number of fibres 100). In (b), the length of the fibre is further constrained by a randomly chosen length (number of fibres 1000).

Filter modelling

For the case of the filter structure, calculations have been carried out to determine the scaling behaviour in terms of the perimeter fractal dimension of the remaining surface area of a filter, that is of a two-dimensional object with holes which represent the filter pores. This approach is thus similar to those used for deposit rate and properties modelling given above, but requires a distinctly different treatment and range of resolution. This part of the calculation procedure has been verified by comparison with a known theoretical case (Sierpinski).

To provide some test data, mathematically simulated filters were created to represent fibrous membrane filters and generated by random processes limited by defined sets of constraints. Comparison of the known theoretical fractal dimension (1.89) with that generated by the procedure (1.92) confirmed that the approach is valid. Since the Sierpinski fractal is known to be similar to some industrial membrane filters, additional data for a real high-temperature ceramic filter were produced from a digitised SEM image of a cross-section. This gave a value of 1.78 which compares favourably with the values of 1.577 and 1.810 for the corresponding artificially generated filters, shown in Fig. 9, and are remarkably similar to some industrial filter sections.

Recent work has included modelling of the deposition processes in an electrostatic precipitator using cellular automata models near the walls of the filter, with characterisation of deposit structure using a fractal analysis. The experimental tests on the bulk-particle-laden flow within the electrostatic precipitator are described in the following section. The models are tested by comparison with the physical experiments.

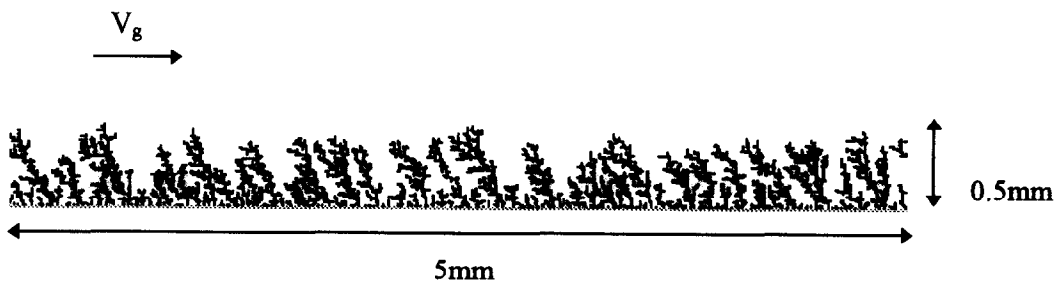


Fig. 10. Simulation of fouling in the boundary layer region of an electrostatic precipitator. The particles enter the boundary layer from above and are carried by a gas velocity (V_g) of 0.95 ms^{-1} from left to right until they are either deposited or carried out of the region. Here the grid size is 500×50 and the particles $10 \mu\text{m}$ diameter: 10 000 particles were released and 5121 deposited. Particles velocities were drawn from a uniform distribution between 0 and 1. The relative magnitude of the deposition forces was

$$F_{\text{drag}}/F_{\text{electric}} \approx 3.0, F_{\text{drag}}/F_{\text{inertia}} \approx 15.0 \text{ and } F_{\text{drag}}/F_{\text{diffusion}} \approx 12.0.$$

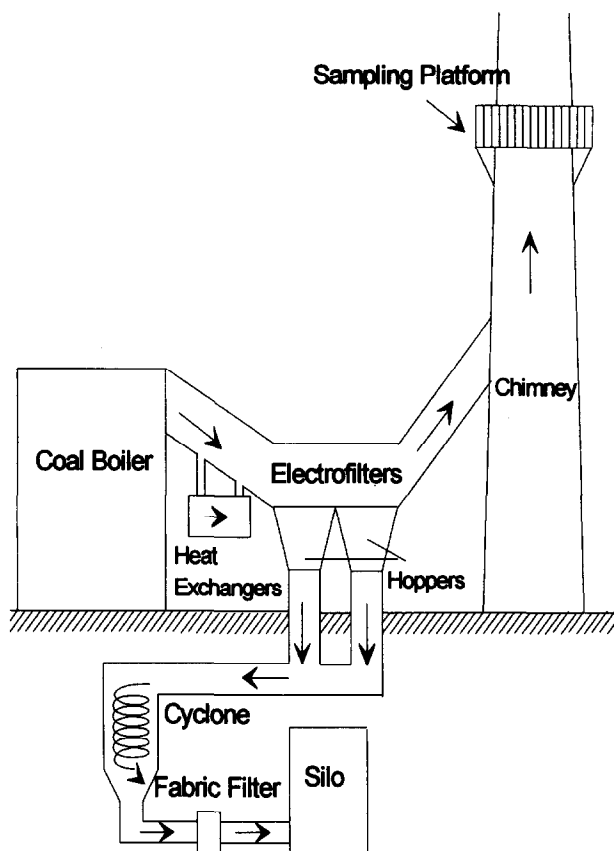


Fig. 11. Boiler plant with electrostatic precipitator.

The simulation included the effects of the electric field, the hydrodynamic drag force on the particle, its inertia and diffusional forces. The particle diameter was $10\ \mu\text{m}$ with a boundary layer width of $0.5\ \text{mm}$. A typical simulated deposit is shown in Fig. 10, along with the parameters used for its generation.

Filter experiments

The objective of the study carried out at GRETh has been to perform dust emission and gas properties measurements on a coal boiler plant downstream of an industrial electrostatic filter to determine its efficiency. The plant is shown schematically in Fig. 11 and consisted of a twin-grate 27 MW urban boiler, with an estimated gas flow rate of $40\ 000\ \text{m}^3\text{h}^{-1}$ at normal pressure and temperature.

Isokinetic samples of dust emissions have been taken with the aid of an industrial partner, Centre Technique des Industries Aerauliques et Thermiques (CETIAT), and measurements made of gas velocity across several test sections downstream of the electrofilter. The average gas stream temperature in the stack and the carbon dioxide concentration were also monitored with time. In addition, the dust samples were analysed using a scanning electron microscope (SEM) and X-ray analysis, in collaboration with CEREM, Centre d'Etudes et de Recherches sur les Matériaux.

Preliminary analysis of the dust samples has shown that essentially three different types of deposit can be identified. These are physically different in structure and have been provisionally characterised as:

- Spheres: composed mainly of silica, aluminium and iron.
- Platelets: composed mainly of sulphur, silica and phosphorus.
- 'Gruyere': composed mainly of silica potassium and zinc.

CONCLUSIONS

As a result of the opportunities which this study provided it has been possible to produce useful new methods or results for several specialised areas linking fouling, combustion and filters. These results, along with more detailed conclusions, have been or will be published more fully elsewhere (at least six additional publications from the contributors are in preparation), but the examples provided here illustrate a few of the significant contributions. Both sets of results for bulk and near wall furnace modelling have provided detailed information on the behaviour of particulate material and, for the bulk case, particulate formation, which may be used to help optimise performance. Similarly the deposit and filter simulations have produced mathematically characterised results which are closely related to the measured values found in real systems, thus improving our understanding of the processes involved. Extensive measurements have also been carried out using specially developed probes and standard techniques, in both industrial furnace and filtration environments, and these, along with deposit chemical analyses, have provided data to validate the theoretical studies. Application of these in appropriate industries will contribute to improved energy efficiency.

Acknowledgements—The authors would like to acknowledge the contributions of the other participants in the project from the organisations listed in the introduction. Part financing by the Commission of the European Communities within the JOULE II Programme—Rational Use of Energy in Industry, is also gratefully acknowledged.

REFERENCES

1. D. E. Rosner, *Transport Processes in Chemically Reacting Systems*. Butterworths, Boston (1986).
2. J. L. T. Azevedo, A. J. Branco, M. G. Carvalho and C. F. M. Coimbra, NO_x emissions from a front wall fired pulverised coal boiler. *Energy Efficiency in Process Technology* (Edited by P. A. Pilavachi). Elsevier Applied Science, London and New York, pp. 872–882 (1992).
3. J. D. Isdale, Generic studies for industrial heat exchanger fouling. *Energy Efficiency in Process Technology* (Edited by P. A. Pilavachi). Elsevier Applied Science, London and New York, pp. 715–725 (1992).
4. J. D. Isdale, P. Mercier, J. M. Grillot, A. Mulholland and J. Gomatam, Integrated modelling of process heat transfer with combustion and fouling. *Applied Thermal Engng.* **17**, 751–762 (1997).
5. M. Soltani and G. Ahmadi, Direct numerical simulation of particle entrainment in turbulent channel flow. *Phys. Fluids* **7**, 3, 647–657 (1995).
6. B. E. Launder and D. B. Spalding, *Mathematical Models of Turbulence*. Academic Press, New York (1972).
7. P. Mercier and M. Villand, The multi-dimensional thermohydraulic code TRIO—application to heat exchangers. *Proc. Eurotherm Seminar No. 18, Design and Operation of Heat Exchangers*, Hamburg (1991).
8. M. Tassopoulos, Relationship between particle deposition mechanism, deposit microstructure and effective transport properties. PhD thesis, Yale University (1991).
9. J. F. Thovert, F. Wary and P. M. Adler, Thermal conductivity of random media and regular fractals. *J. Appl. Phys.* **68**, 8, 3872–3883 (1990).
10. P. M. Adler and J. F. Thovert, Fractal porous media. *Transport in Porous Media* **13**, 41–78 (1993).
11. A. J. Mulholland, C. MacDonald, S. McDermott, B. Manimala and J. Gomatam, Calculation of the effective thermal conductivity of fractal deposits (in preparation).
12. D. S. Ensor and M. E. Mullins, The fractal nature of dendrites formed by the collection of particles on fibres. *Part. Charact.* **2**, 77–78 (1985).
13. D. Houi and R. Lenormand, Particle deposition on a filter medium. In *Kinetics of Aggregates and Gelation*. (Edited by F. Family and D. P. Lenormand) Elsevier, Amsterdam (1994).
14. P. Schmitz, D. Houi and B. Wandelt, Hydrodynamic aspects of crossflow microfiltration. Analysis of particle deposition at the membrane surface. *J. Membrane Sci.* **71**, 29–40 (1992).
15. M. Tassopoulos, J. A. O'Brien and D. E. Rosner, Simulation of microstructure/mechanism relationships in particle deposition. *AIChE J.* **35**, 6, 967–980 (1989).